Sodium butyrate ameliorates insulin resistance and renal failure in CKD rats by modulating intestinal permeability and mucin expression

Austin Gonzalez[1], Richard Krieg[2], Hugh D. Massey[3], Daniel Carl[1], Shobha Ghosh[4], Todd W.B. Gehr[1] and Siddhartha S. Ghosh[1]

[1]Department of Internal Medicine, Nephrology, Virginia Commonwealth University, Richmond, VA, USA, [2]Department of Anatomy, Virginia Commonwealth University, Richmond, VA, USA, [3]Department of Pathology, Virginia Commonwealth University, Richmond, VA, USA and [4]Department of Internal Medicine, Pulmonary and Critical Care, Virginia Commonwealth University, Richmond, VA, USA

Correspondence and offprint requests to: Siddhartha S. Ghosh; E-mail: siddhartha.ghosh@vcuhealth.org

ABSTRACT

Background. The associated increase in the lipopolysaccharide (LPS) levels and uremic toxins in chronic kidney disease (CKD) has shifted the way we focus on intestinal microbiota. This study shows that a disruption of the intestinal barrier in CKD promotes leakage of LPS from the gut, subsequently decreasing insulin sensitivity. Butyrate treatment improved the intestinal barrier function by increasing colonic mucin and tight junction (TJ) proteins. This modulation further ameliorated metabolic functions such as insulin intolerance and improved renal function.

Methods. Renal failure was induced by 5/6th nephrectomy (Nx) in rats. A group of Nx and control rats received sodium butyrate in drinking water. The Nx groups were compared with sham-operated controls.

Results. The Nx rats had significant increases in serum creatinine, urea and proteinuria. These animals had impaired glucose and insulin tolerance and increased gluconeogenesis, which corresponded with decreased glucagon-like peptide-1 (GLP-1) secretion. The Nx animals suffered significant loss of intestinal TJ proteins, colonic mucin and mucin 2 protein. This was associated with a significant increase in circulating LPS, suggesting a leaky gut phenomenon. 5'adenosine monophosphate-activated protein kinase (AMPK) phosphorylation, known to modulate epithelial TJs and glucose metabolism, was significantly reduced in the intestine of the Nx group. Anti-inflammatory cytokine, interleukin 10, antibacterial peptide and cathelicidin-related antimicrobial peptide were also lowered in the Nx cohort. Butyrate treatment increased AMPK phosphorylation, improved renal function and controlled hyperglycemia.

Conclusions. Butyrate improves AMPK phosphorylation, increases GLP-1 secretion and promotes colonic mucin and TJ proteins, which strengthen the gut wall. This decreases LPS leakage and inflammation. Taken together, butyrate improves metabolic parameters such as insulin resistance and markers of renal failure in CKD animals.

Keywords: chronic renal failure, diabetic kidney disease, gut, nephrectomy, short chain fatty acid

INTRODUCTION

Intestinal dysbiosis is a phenomenon seen in chronic kidney disease (CKD) patients and also in animal models of CKD [1–3]. Dysbiosis is also implicated in diabetes [4], a disease frequently associated with CKD. Uremia significantly contributes to dysbiosis and alters the biochemical environment of the gut. Cumulatively, this can lead to the alteration of tight junction (TJ) proteins of the intestinal epithelial cells. Disruption of intestinal TJ proteins following CKD leads to leakage of various toxic biomolecules, including phenols, cresols, lipopolysaccharides (LPS), etc., from the gastrointestinal tract to the systemic circulation [2, 5, 6]. Enhanced absorption of these biomolecules can also aggravate uremia along with associated diseases such as diabetes.

Gut microbiota, intestinal TJ proteins and intestinal mucin together play a key role in keeping bacteria and bacterial end products within the intestine. Although changes in gut microbiota and intestinal TJ proteins in CKD have been well explored [1, 6–8], there is a paucity of information regarding intestinal mucin in renal failure. The intestine is protected by mucus and in the colon it forms a double layer. The major building blocks giving mucus its properties are large glycoproteins, called mucins, that prevent bacterial translocation from the intestine [9]. In a recent study, increased translocation of bacteria and endotoxins into the liver and systemic circulation, respectively,

has been demonstrated in animals with renal failure [10]. In addition to its protective barrier function against microbes, mucus also prevents other toxic and noxious substances from reaching the epithelial surface [11]. The mucin layer also provides the matrix for the retention of antimicrobial molecules that helps to control the microbial content of the gut [12].

The colon harbors significant populations of bacteria that include butyrate-producing species. Microbial fermentation in the gut plays an important role in gut homeostasis and has an impact on host metabolism and health [13, 14]. Short-chain fatty acids (SCFAs), such as butyrate, are bacterial fermentation products. They are absorbed by the gastrointestinal epithelial cells of the colon and rapidly oxidized for adenosine triphosphate synthesis, thus providing nutrition to the colon [15]. Butyrate is not only a nutrient for the colonocytes but also has been shown to promote reassembly of intestinal TJ proteins [16] and improve gut barrier function by promoting mucin synthesis [17]. A significant positive correlation has been shown between fecal butyrate levels and ammonia excretion [13]. Butyrate also possesses significant anti-inflammatory and antioxidant properties [15] and has been shown to improve insulin sensitivity and diabetes control in mice [18, 19]. More importantly, the abundance of SCFA-producing bacteria is reduced in patients with end-stage renal disease (ESRD) [20].

Interventions that improve intestinal symbiosis, neutralize bacterial endotoxins or adsorb gut-derived uremic toxins are being developed to help assuage CKD [21]. Some probiotics have been shown to improve the control of diabetes by increasing glucagon-like peptide-1 (GLP-1) hormone secretion via butyrate [22]. Preliminary clinical trials have shown that elevating GLP levels may improve kidney function in patients with diabetes [23, 24]. In addition, a diet rich in indigestible and fermentable complex carbohydrates encourages SCFA production by the gut microbiome and has been shown to alleviate CKD in animal models [25, 26].

5/6th nephrectomy (Nx) is a widely used model for studying glomerulosclerosis and translates to CKD as a result of nephron loss in humans [27]. These animals have intestinal dysbiosis [3], hyperglycemia, insulin resistance and increased hepatic gluconeogenesis [28, 29]. Since butyrate is known to stimulate GLP-1 secretion [30] and modulate TJ proteins, we designed this study to understand if butyrate, by modulating intestinal permeability and mucin secretion, could ameliorate diabetes and improve renal failure in CKD animals.

MATERIALS AND METHODS

Sodium butyrate was purchased from Sigma Chemicals (St. Louis, MO, USA). Antibodies [cathelicidin-related antimicrobial peptide (CRAMP), CaMMKβ, β-actin and sodium potassium ATPase] were purchased from Santa Cruz Biotechnology (Dallas, TX, USA). Antibodies (ZO-1 and Claudin-1) were purchased from Thermo Fisher Scientific (Waltham, MA, USA). Antibodies (pAMPK, AMPK) were purchased from Cell Signaling Technology (Danvers, MA, USA).

Animals

All animal procedures were approved by the Institutional Animal Care and Use Committees of Virginia Commonwealth University.

Rats were divided into four groups. The control group ($n = 6$) had sham surgery and ad libitum drinking water. A cohort of rats ($n = 5$) were sham operated and given butyrate in the drinking water (butyrate control). Twelve rats, divided equally, underwent 5/6th Nx by the procedure described below. One group of Nx animals was given 400 mg/kg/day sodium butyrate in drinking water (Nx + butyrate; $n = 6$) and the other six Nx rats did not receive any treatment (Nx). Each rat was housed in a single cage to monitor the water consumption of individual rats. Water intake was monitored for every 2 days. Based on the water intake, the dose of sodium butyrate was adjusted so that the butyrate consumption was 400 mg/kg/day.

Surgery

CKD was induced in rats by the method published previously by Ghosh *et al.* [31]. 5/6th Nx of rats weighing between 150 and 200 g was performed using a sterile technique. All operations were carried out under isoflurane anesthesia. A left flank incision was made and the left kidney was exposed. The renal artery was temporarily occluded and the upper and lower thirds of the kidney were ligated and excised. Bleeding was controlled by compression until it stopped. Thus one-third of the mass of the left kidney remained. The muscle and skin incisions were sutured with polypropylene sutures. The animals were returned to the vivarium to recover. One week later a right flank incision was made, the renal vessels and ureter were ligated and the right kidney was excised. Animals were returned to the vivarium to recover. Animals were kept in metabolic cages after 14 days. Urine was collected and urinary protein and creatinine measured to verify renal failure. At the end of 8 weeks after the second surgery, an oral glucose tolerance test (GTT) was done. Four days later animals were subjected to the pyruvate tolerance test (PTT) and four days after PTT the insulin tolerance test (ITT) was done. After this, the animals were sacrificed.

GTT, PTT and ITT

GTT, PTT and ITT were measured by methods described in the literature [28, 29]. For GTT and PTT, animals were fasted overnight. For GTT, animals were given glucose orally at a dose of 2 g/kg body weight (Sigma, St. Louis, MO, USA). For PTT, sodium pyruvate (Sigma; 2 g/kg) was injected intraperitoneally (i.p.). Blood glucose (tail clip) was measured by a glucometer at 0–120 min and additional blood was collected. For ITT, animals were fasted for 6 h and injected i.p. with 1.0 unit/kg Humulin R. Blood glucose (tail clip) was measured by glucometer at 0–60 min.

Plasma GLP-1

Rats were given 2 g/kg glucose and blood was collected in the presence of protease and dipeptidyl peptidase 4 inhibitor (MilliporeSigma, St. Louis, MO, USA). The GLP-1 assay was done by an enzyme-linked immunosorbent assay kit (Sigma) using the manufacturer's information.

A. Gonzalez *et al.*

Plasma LPS

Plasma LPS was assayed as described earlier [32]. Trunk blood from the rats was collected at the time of sacrifice and plasma was frozen at −80°C until it was analyzed. Plasma LPS levels were determined by the Endpoint Chromogenic LAL assay (Lonza, Walkersville, MD, USA) according to the manufacturer's instructions, with the following modifications: samples were diluted 5- to 10-fold to avoid interference with background color and preheated to 70°C for 10 min prior to analyses.

Tissue processing

The colon, duodenum and ileum were isolated at necropsy and stored at −80°C. Although most of the experiments were done with the colon, all tissues were homogenized with a Dounce homogenizer and membrane nuclear and cytosolic fragments were isolated and stored at −80°C. For the colon section, the first 2 cm of the ascending colon was cut for histology and the next 4 cm was cut and stored at −70°C for immunoblot processing.

The colon sections were fixed in methacarn (methanol, 60 mL; chloroform, 30 mL; acetic acid glacial, 10 mL) and transferred to 95% ethanol after 24 h. They were then transferred to Histoclear (Fisher Scientific, Waltham, MA, USA) and then were submitted to paraffin embedding and sectioning. From that point, Alcian blue and immunohistochemistry were feasible.

Isolation of membrane protein from tissue

The Mem-PER Plus Kit (Thermo Fisher Scientific) was used to isolate membrane proteins according to the manufacturer's protocol.

Isolation of nuclear and cytosol fraction from tissue

Homogenization was carried out as described earlier [31]. The frozen tissues were pulverized in ice-cold 4-(2-hydroxyethyl)-1-piperazineethanesulfonic acid (HEPES) buffer [10 mM HEPES, 0.2% Triton X-100, 50 mM NaCl, 0.5 mM sucrose, 0.1 mM ethylenediaminetetraacetic acid (EDTA), protease and phosphatase inhibitors) and homogenized with an ice-chilled Dounce homogenizer at 4°C. An aliquot of the homogenate was stored and the rest was used to make cytosolic and nuclear extracts. This was spun at 10 000 rpm for 10 min and the supernatant was aliquoted and stored at −70°C as 'cytosolic extract'. The pellet was suspended in ice-cold buffer (10 mM HEPES, 500 mM NaCl, 10% glycerol, 0.1 mM EDTA, 0.1 mM ethyleneglycotetraacetic acid, 0.1% IGEPAL and protease and phosphatase inhibitors) and vortexed at 4°C for 15 min and centrifuged for 10 min at 14 000 rpm. The resulting supernatant was aliquoted and stored as 'nuclear extract' at −70°C. Absence of cross-reactivity with β-actin in western blots confirmed the purity of nuclear extracts. A small aliquot of kidney homogenate, along with cytosol and nuclear extract, was kept at 4°C for protein estimation.

Immunoblotting

Colon cytosol (75–100 μg total protein) and nuclear extracts (50 μg total protein) were separated on a 4–20% sodium dodecyl sulphate–polyacrylamide gel electrophoresis gel and proteins were transferred to a Polyvinylidene difluoride membrane. Western blots were carried out using different antibodies as described earlier [33].

Immunohistochemistry

Mucin 2 (Muc2) antibody (Santa Cruz Biotechnology) was used to detect Muc2 expression in rat colon. Colon sections were deparafinized and antigen retrieval done using sodium citrate buffer. After blocking with 5% serum for 1 h, the sections were immunostained overnight at 4°C with rabbit anti-rat Muc2 antibody. After being washed with phosphate-buffered saline, they were treated with diluted biotinylated secondary anti-rabbit antibody (1:50; Vector Labs, Burlingame, CA, USA) for 60 min at room temperature. This was followed by incubation with neutravidin conjugated to fluorescent probes (Molecular Probes, Invitrogen, Carlsbad, CA, USA). Images were acquired using an Olympus inverted microscope fitted with a digital camera and analyzed with ImageJ software (https://imagej.nih.gov).

Alcian blue stain for mucin

Alcian blue is known to stain mucin [34]. After dewaxing and hydration, the colon sections were exposed to Alcian blue stain for 30 min at room temperature. The excess solution was rinsed with running tap water. The sections were dehydrated and mounted.

Image analysis

The staining was assessed by ImageJ software (https://imagej.nih.gov), setting a 'threshold' using the thresholding tool. The threshold was adjusted until all stained areas were selected. 'Limit to threshold' was selected and the set areas measured [35]. Four fields were taken for each image. The investigator doing this analysis was blinded and results were reconfirmed by another investigator in a blind fashion. The data from both the investigators were averaged. Although care was taken to process all the slides at one time, immunostains are not stoichiometric, hence the data represented are semiquantitative.

Renal biochemistry

Serum urea. The QuantiChrom Urea Assay Kit (Fisher Scientific, Waltham, MA, USA) was used to measure serum urea. The assay was carried out according to the manufacturer's protocol.

Serum creatinine. A Bioassay Systems (Fisher Scientific, Waltham, MA, USA) creatinine assay kit was used to measure serum creatinine. The assay was carried out according to the manufacturer's protocol.

Proteinuria. Urinary protein was measured by a bicinchoninic acid protein assay.

RESULTS

5/6th Nx was carried out in rats to generate CKD. Disruption of TJ proteins and gut microbiota has been observed in the 5/6th

Nx CKD rat model [7, 8]. In addition to renal failure and changes in intestinal permeability, Nx rats develop insulin resistance and hyperglycemia [28, 29]. The following results show the effect of butyrate on hyperglycemia, intestinal permeability and renal failure in this CKD rat model.

Impaired GTT, gluconeogenesis (PTT) and reduced insulin sensitivity (ITT) in Nx (CKD) rats improved by butyrate

It has been demonstrated that both glucose tolerance and insulin tolerance are impaired in CKD patients and in the remnant kidney model of CKD. Fasting blood glucose levels (time point 0) taken before the start of the GTTs were not significantly different among the groups (Figure 1A). However, after oral glucose administration, the plasma glucose levels of the CKD animals were significantly higher than the control (from 15 to 60 min time points) and the butyrate control (from 15 to 30 min time points). There was no significant difference in the glucose levels of the control and butyrate control at any time point. The plasma glucose levels of butyrate-treated CKD animals (Nx + butyrate) were significantly lower than untreated CKD (Nx) between 15 and 60 min (Figure 1A). There was no significant difference between the glucose levels of control and butyrate control groups (Figure 1A). The overall glucose area under the curve (AUC) of the CKD (Nx) cohort was significantly higher than the control ($P < 0.01$) and butyrate control ($P < 0.01$). As shown in Figure 1B, the plasma glucose AUC of the butyrate-treated group had significantly improved glucose tolerance ($P < 0.05$). Between the control, butyrate control and butyrate-treated Nx groups (Nx + butyrate) there was no significant difference in the glucose AUC.

The ITT clearly showed that the plasma glucose levels of the Nx group, after insulin injection, were significantly higher than the control and butyrate control from 30 min onwards (Figure 1C). Also shown in Figure 1C, there was no significant difference between the glucose levels of the control and butyrate control groups. Our data show that insulin treatment failed to control the plasma glucose in CKD animals, suggesting insulin resistance. From the 30-min time point onwards, the CKD cohort treated with butyrate (Nx + butyrate) showed a significant reduction in plasma glucose, suggesting that butyrate improves insulin sensitivity. As shown in Figure 1D, the plasma glucose AUC of the Nx group after insulin injection was significantly higher than the control ($P < 0.05$) and butyrate-treated groups ($P = 0.004$). Butyrate treatment significantly abrogated the increase in the glucose AUC ($P < 0.05$). There was no significant difference between the glucose AUC of the control and butyrate control groups. The glucose AUC of butyrate-treated CKD animals (Nx + butyrate) was not significantly different from either the control or the butyrate-treated controls.

The PTT is a measure of gluconeogenesis and as shown in Figure 1E, the blood glucose levels of the CKD cohort at 15 and 30 min after pyruvate administration were significantly higher than the control and butyrate control ($P < 0.05$ and 0.01, respectively). At the 15 and 30 min time points, the butyrate-treated CKD (Nx + butyrate) group had significantly lower plasma glucose levels compared with the untreated CKD (Nx)

group (Figure 1E). In the CKD group, the blood glucose AUC following pyruvate administration was significantly higher than the control ($P = 0.0019$) and butyrate control ($P = 0.0094$), suggesting increased gluconeogenesis in Nx animals, which may contribute to the hyperglycemia seen in this cohort. The blood glucose AUC in the Nx + butyrate group was 20% lower than in the CKD cohort ($P = 0.023$; Figure 1F), suggesting that butyrate impedes increased gluconeogenesis in CKD animals. Pyruvate treatment did not produce a significant difference in the glucose levels between the control and the butyrate-treated control groups. No significant difference in the glucose AUC was observed between the control group, butyrate control group and butyrate-treated Nx cohort (Nx + butyrate).

Decreased levels of plasma GLP-1 in the Nx (CKD) cohort were reversed with butyrate treatment

Butyrate has been shown to stimulate GLP-1 secretion, hence it is possible that the antidiabetic effect of butyrate is mediated via GLP-1 secretion. To determine if GLP-1 levels are altered in animals with renal failure, oral glucose was given (as described in the methods) to all the groups to stimulate GLP-1 secretion. The Nx group had approximately 30% lower plasma GLP-1 than the control and butyrate control groups ($P = 0.0452$ and 0.0323, respectively). As shown in Figure 2A, there was a significant increase in serum GLP-1 in the Nx animals after butyrate treatment. The GLP-1 levels of the Nx + butyrate cohort were almost 2-fold higher than the untreated Nx group ($P = 0.007$). Plasma GLP-1 levels of the control and butyrate control groups were not significantly different. The plasma GLP-1 levels of the control, butyrate control and Nx + butyrate groups were not significantly different.

Increased circulating LPS in Nx (CKD) animals abated by butyrate treatment

Circulating levels of LPS in Nx animals (Figure 2B) were 3-fold higher than the control and butyrate control groups ($P < 0.0001$). This increase in endotoxemia may contribute not only to hyperglycemia, but also to inflammation associated with CKD. Butyrate treatment significantly reduced circulating LPS levels by 24% ($P = 0.0338$), although the levels of the butyrate-treated Nx group were still higher than the control ($P = 0.005$) and butyrate control ($P = 0.006$) groups. There was no significant difference in plasma LPS between the control and butyrate control groups.

As shown above, physiological parameters such as GTT, ITT, PTT, GLP-1 and LPS of the control and butyrate control groups were not significantly different. Hence only the control group was used as a comparison for further mechanistic studies.

Reduced expression of intestinal TJ proteins ZO-1 and claudin-1 in the colon of Nx (CKD) animals is thwarted by butyrate treatment

The colonic membrane and cytosol were separated and immunoblot analysis showed that compared with controls (Figure 3A), cytoplasmic ZO-1 was significantly lower in the Nx group ($P < 0.01$) and butyrate treatment blocked this
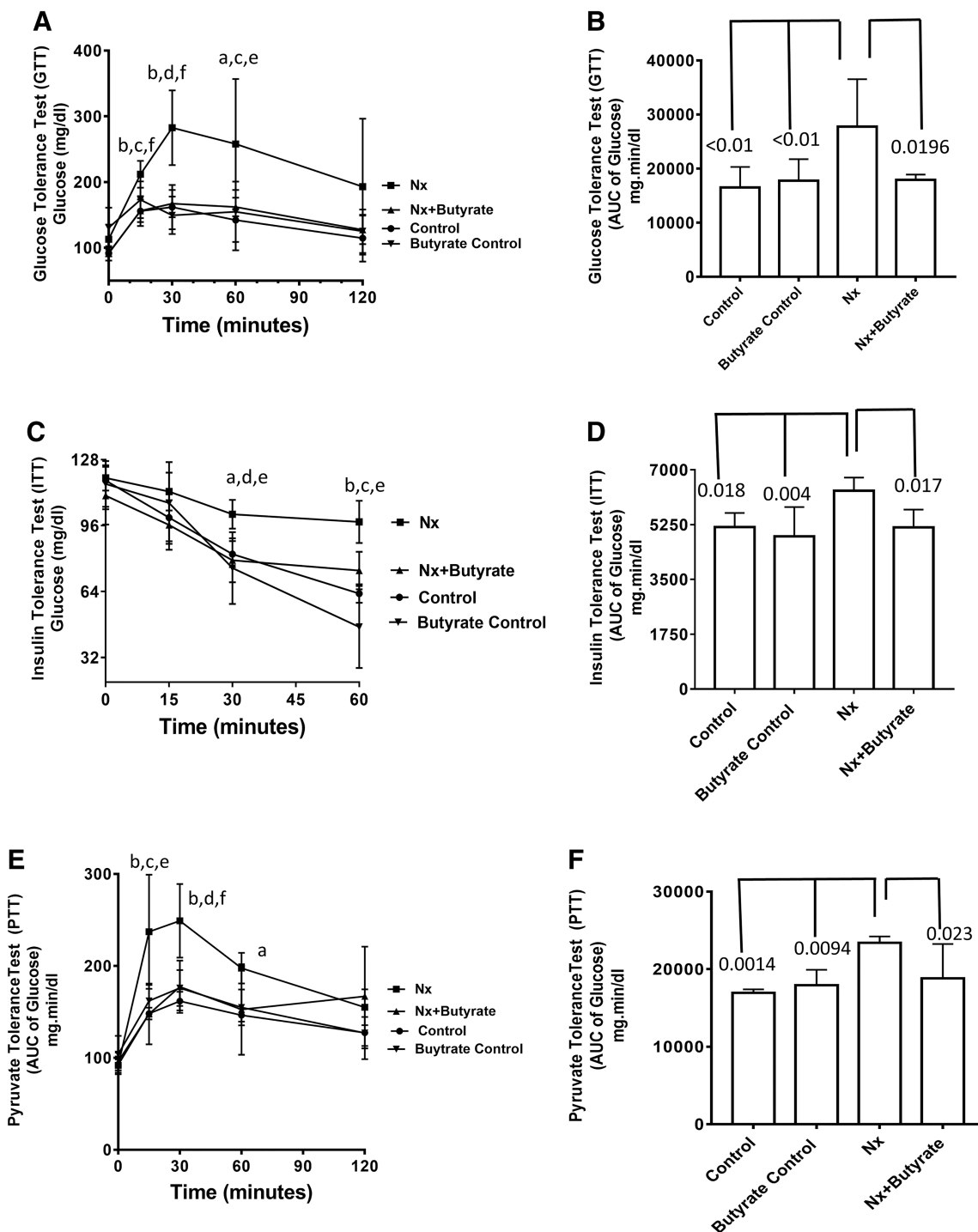
A. Gonzalez *et al.*

FIGURE 1: Butyrate ameliorates hyperglycemia in 5/6th Nx rats. Butyrate treatment was started 2 weeks after surgery and continued for 6 weeks. **(A)** Oral GTT: Plasma glucose concentration in response to oral glucose administration. **(B)** AUC of glucose after oral glucose administration. **(C)** ITT: The animals were given insulin i.p. and plasma glucose measured by glucometer. **(D)** AUC of glucose after insulin administration. **(E)** PTT: Plasma glucose concentration in response to i.p. pyruvate administration. **(F)** AUC of glucose after pyruvate administration. Data are expressed as mean $\pm$ SD ($n = 6$). Butyrate control consisted of five animals. Statistically significant differences between the groups are given as follows: [a]P < 0.05 compared with control; [b]P < 0.01 compared with control; [c]P < 0.05 compared with butyrate control; [d]P < 0.01 compared with butyrate control; [e]P < 0.05 compared with Nx + butyrate; [f]P < 0.01 compared with Nx + butyrate.
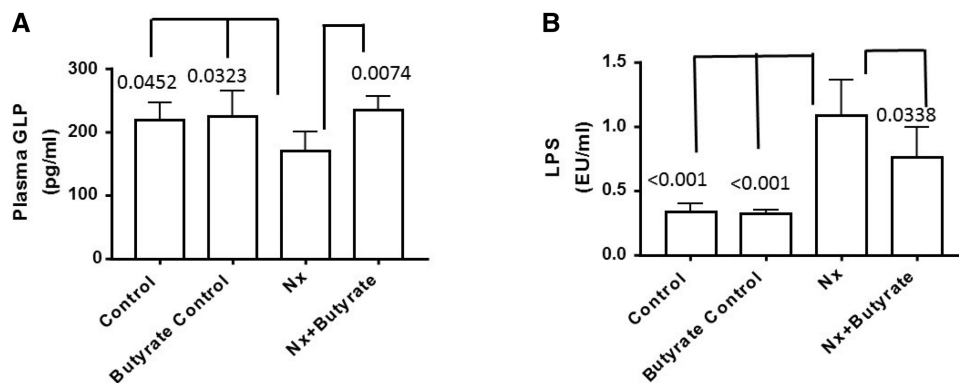
FIGURE 2: Butyrate increases GLP-1 secretion and reduces plasma LPS levels of 5/6th Nx rats. Butyrate was given for 6 weeks. **(A)** Blood was collected 8 weeks after surgery. Plasma GLP was measured by enzyme immunoassay 30 min after oral glucose administration (2 g/kg). GLP levels of the Nx group were significantly lower than the control and butyrate control groups. Butyrate treatment significantly abated the decrease. There was no significant difference in the GLP levels of the control, butyrate control and Nx + butyrate groups. **(B)** Plasma LPS was measured by a Lonza kit. The LPS levels of the Nx group were significantly higher than the control and butyrate control groups. Although butyrate treatment (Nx + butyrate) significantly decreased the LPS levels, it was still significantly higher than the control ($P = 0.005$) and butyrate control ($P = 0.006$) groups. Data are mean ± standard deviation of five to six animals per group. Butyrate control consisted of five animals.

decrease. There was no significant difference in the ZO-1 protein between the control and Nx + butyrate groups. In the cytosol, claudin-1 could be detected in only three of six animals and no differences were observed between the groups. However, the membrane subcellular fraction of the colon showed that the Nx group had 25% lower claudin-1 than the control group ($P = 0.0484$) and butyrate treatment abrogated the reduction (Figure 3B). The amount of cytosolic and membrane claudin protein was not significantly different between the control and Nx + butyrate groups. ZO-1 proteins could not be detected in the membrane.

Decrease in AMPK phosphorylation and calmodulin-dependent protein kinase in the colon of Nx (CKD) animals is abrogated by butyrate treatment

To understand if intestinal AMPK plays a role in CKD, we measured the AMPK levels in the colon by western blot. As shown in Figure 4A, the Nx group had 55% lower phosphorylated AMPK ($P = 0.0117$) and butyrate treatment significantly augmented AMPK phosphorylation ($P = 0.0169$). No significant difference in AMPK phosphorylation was observed between the control and Nx + butyrate groups. The colonic calcium/calmodulin-dependent protein kinase kinase beta (CaMKKβ) of the Nx group (Figure 4B) was significantly lower than in the control group, and butyrate treatment significantly improved CAMKKβ levels ($P = 0.003$). The colonic CaMKKβ of the control and Nx + butyrate groups was not significantly different.

Reduced mucin expression in the colon of Nx (CKD) animals improved by butyrate treatment

To determine if colonic mucin is altered in renal failure, we stained the colons with Alcian blue (Figure 5), a dye known to stain mucin. Compared with the controls, mucin expression in the Nx animals was significantly reduced by almost 50% ($P < 0.001$). There was a significant reduction of mucin in the goblet cells. It has been shown that sodium butyrate treatment increases colonic mucin synthesis and in this study, as demonstrated by Alcian blue staining, Nx animals treated with butyrate had significant improvement (1.5-fold increase) of colonic mucin ($P < 0.05$). Mucin levels in the control colon and butyrate-treated Nx colon (Nx + butyrate) were not significantly different.

Lowered Muc2 expression in the colon of Nx (CKD) animals is antagonized by butyrate

Mucins are the major components of the mucus secreted by goblet cells to protect the intestine. Alcian blue can stain all mucins, especially acidic mucin. However, the most prominent mucin expressed and secreted in the colon is Muc2. Our immunohistochemistry data (Figure 6) show that Muc2 expression in the colon of Nx animals was reduced by 30% ($P < 0.01$) and butyrate treatment significantly improved Muc2 expression ($P < 0.05$). Muc2 levels in the control colon and butyrate-treated Nx colon (Nx + butyrate) were not significantly different.

Loss of colonic interleukin 10 (IL-10) and cathelicidin-related antimicrobial peptide in Nx CKD rats are abated by butyrate

The intestine can produce multiple antimicrobial peptides that keep the gut bacteria under control. Cathelin-related antimicrobial peptide (CRAMP) is one such antimicrobial peptide protein known to be induced by butyrate and is produced in the rat intestine. In this study we found a severe decrease in IL-10 protein in the colon of Nx animals (Figure 7A), which was partially restored by butyrate treatment ($P = 0.017$) but was still significantly below the control ($P < 0.001$). Expression of CRAMP was studied in both the colon and duodenum. In this study, 50% of the animals in the Nx group had undetectable expression of CRAMP in the colon. As shown in Figure 7B, colonic CRAMP was significantly lower than in the controls ($P < 0.0001$), which was significantly increased by butyrate treatment ($P = 0.006$). However, the colonic CRAMP of the
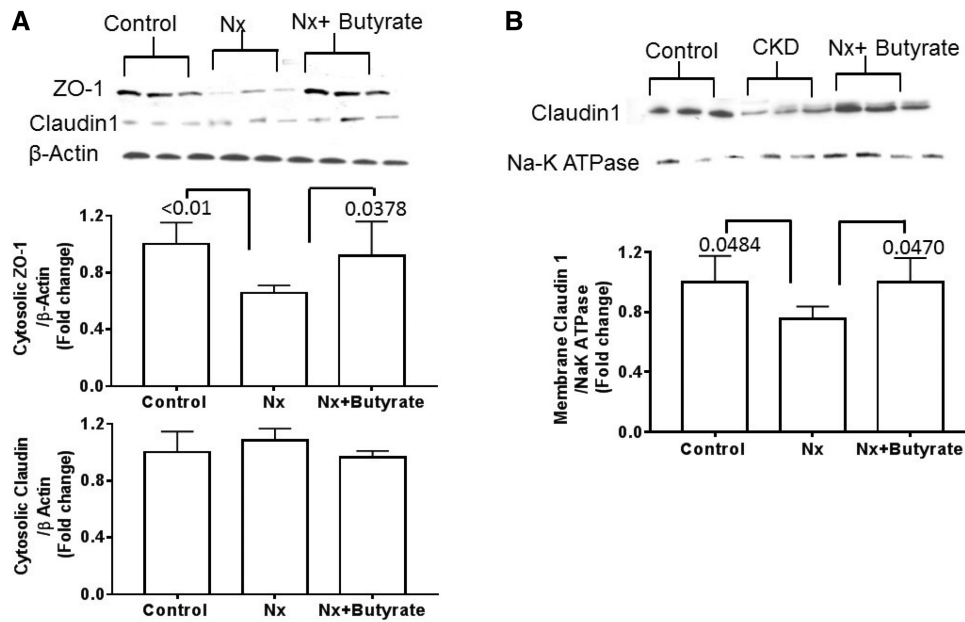
FIGURE 3: Decreased abundance of colonic TJ proteins of the 5/6th Nx group was reversed by butyrate. Representative western blot of ZO-1 and claudin 1. **(A)** Cytosolic ZO-1 but not claudin 1 was significantly reduced in the Nx group. Butyrate treatment significantly improved ZO-1 expression. **(B)** Reduction of membrane claudin 1 in the Nx group was abrogated by butyrate treatment. ZO-1 protein could not be detected in the membrane fraction. Data are mean ± standard deviation of six animals per group. Cytosolic ZO-1 and membrane claudin 1 of the control and Nx + butyrate groups were not significantly different from each other.
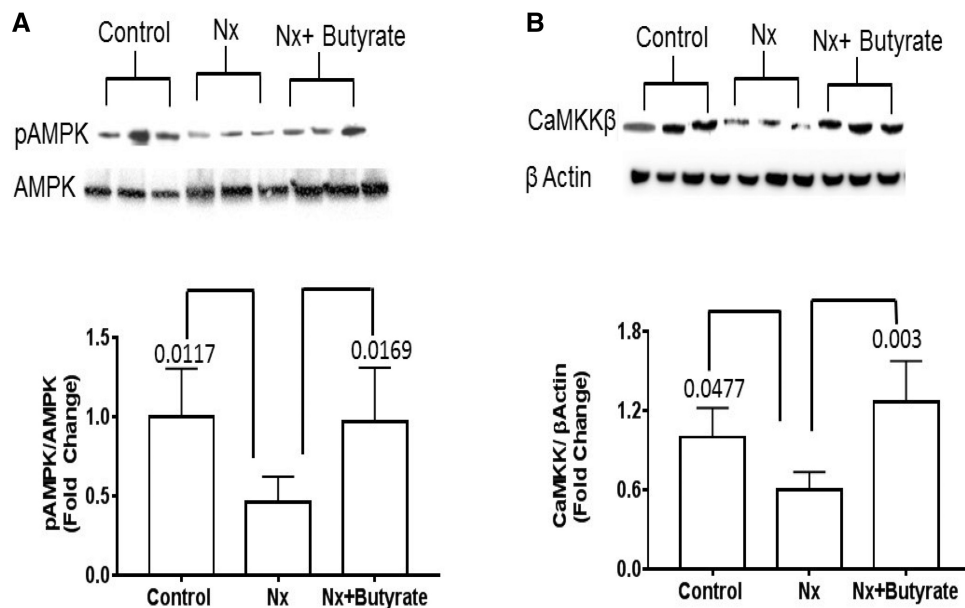

FIGURE 4: Butyrate treatment reverted the decrease in AMPK phosphorylation and CAMKKβ in the colon of Nx animals. **(A)** The representative western blot of phosphorylated AMPK (pAMPK) and AMPK of the colon. A significant decrease in the pAMPK:AMPK ratio in the Nx group was reversed by butyrate treatment. The pAMPK:AMPK ratio between the control and Nx + butyrate groups was not significantly different from each other. **(B)** The representative western blot of CAMKKβ and β-actin of the colon. Reduced CAMKKβ in the Nx colon was reversed by butyrate. Data are mean ± standard deviation of six animals per group. The CAMKKβ between the control and Nx + butyrate groups was not significantly different from each other.

butyrate-treated group (Nx + butyrate) was still higher than in the controls (P < 0.05). In the duodenum, CRAMP was expressed in all three cohorts. Therefore we used the duodenum to assess this protein and found that the expression of CRAMP in Nx animals was significantly lower than in the controls (P < 0.001) but was restored with butyrate treatment (Figure 7C). Although CRAMP is expressed in the colon, in this study, 50% of the animals in the Nx group had undetectable expression of CRAMP in the colon and very low signal in the Nx group. As shown in Figure 7C, butyrate treatment restored it.
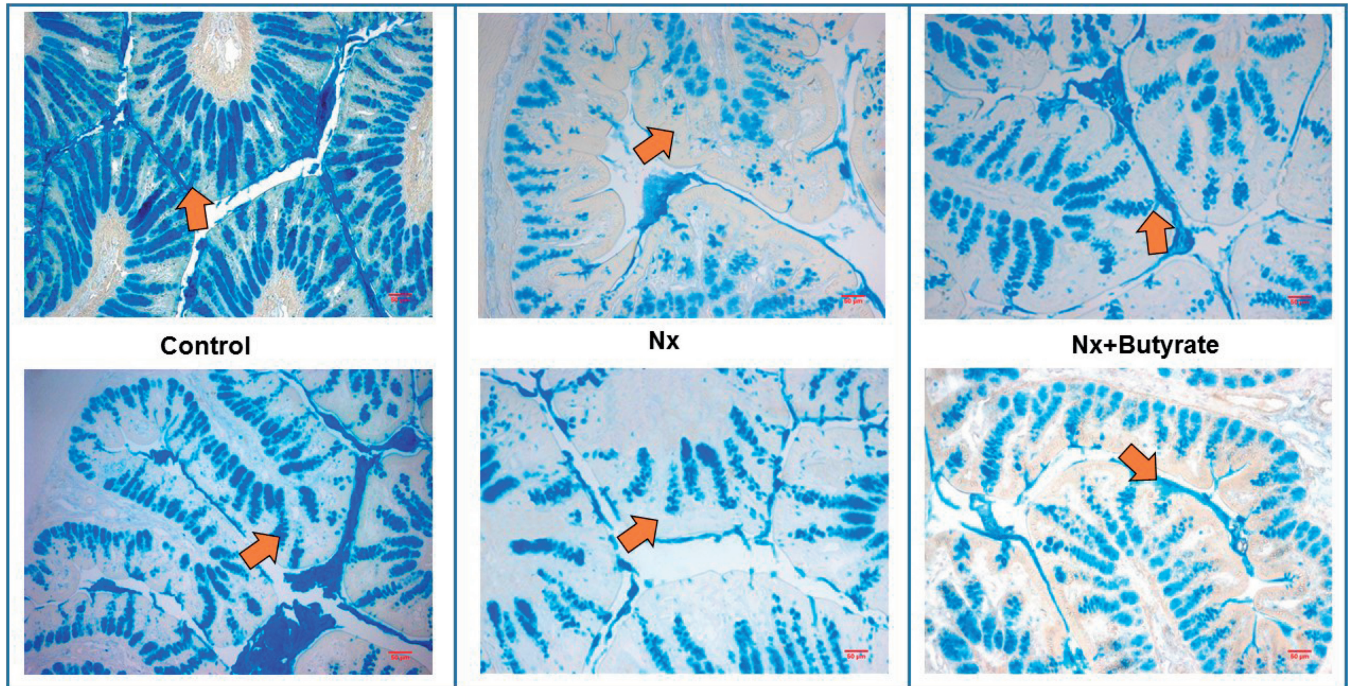
FIGURE 5: Reduced expression of colonic mucin stained by Alcian blue in Nx animals was corrected by butyrate treatment. Representative sections of colonic mucin of two animals from each group (control, Nx and butyrate-treated Nx animals) are shown. The proximal part of the colon (0.5 cm) was collected and stored in Carnoy's solution. Alcian blue stained the mucin in the colon, imparting a blue color under a light microscope ($\times$10 magnification). Please note the decrease in mucin expression of CKD animals (shown by the arrows) and its resurgence following butyrate treatment. Compared with the controls, the blue-stained areas representing mucin expression were significantly less in the Nx groups. Butyrate treatment reversed this effect. A total of six animals per group were used to assess mucin expression.

There was no significant difference in the expression of duodenal CRAMP between the control and Nx + butyrate groups.

Markers of renal failure in 5/6th Nx CKD rats improved with butyrate treatment

As shown in Table 1, the serum urea, urinary protein:creatinine ratio and serum creatinine of Nx rats were significantly higher (3.6-, 3-, and 3.2-fold, respectively) than in sham-operated controls. The serum urea, urinary protein:creatinine ratio and serum creatinine in Nx rats were also significantly higher (3.9, 2.2, and 3.2, respectively) than in the butyrate controls. There was no significant difference in renal biomarkers between the control and butyrate control groups. Butyrate treatment significantly improved proteinuria and serum urea levels. Serum creatinine levels were reduced by 22% with butyrate treatment, but it did not reach statistical significance (P = 0.0504).

These experiments show that decreased colonic mucin and TJ proteins in CKD animals lead to increased paracellular permeability of the uremic toxin LPS. Changes in the intestinal wall can not only be a cause of kidney inflammation, fibrosis and renal failure, but may also play a role in exacerbating insulin resistance. Reinforcing the colon with butyrate can ameliorate insulin resistance and improve renal function.

DISCUSSION

Our study shows 5/6th Nx (CKD) animals had renal insufficiency, hyperglycemia and reduced expression of TJ proteins, mucin and Muc2 in the colon. This was associated with increased plasma LPS and decreased GLP-1. Butyrate-treated Nx animals had marked improvement in all those parameters. Since endotoxemia has been shown to be related to insulin resistance [36], the increased LPS might contribute to the hyperglycemia seen in this study.

Preservation of the mucus layer is involved in safeguarding intestinal permeability. This mucin layer harbors various antimicrobial peptides that keep the bacterial growth in check [12] and a deficiency of mucin can cause enteric colonization of pathogens. Certain pathogens are known to disrupt TJ proteins [37]. Intestinal mucus is produced and secreted by the goblet cells. We saw decreased Alcian blue and Muc2 staining in the goblet cell areas in CKD animals. Moreover, proteins such as trefoil factor 3 and RELM-β, which are required for the maintenance and restitution of the gastrointestinal tract, are enriched in the mucus layer formed by Muc2 [38]. Hence the loss of Muc2 can compromise the integrity of the intestinal TJs, and loss of TJ proteins is observed in CKD [7, 8]. It has been shown that Muc2 mucin and CRAMP may act in concert at the colonic mucosa to support the microbiota and to prevent entry of pathogens [39]. The decreased levels of CRAMP seen in CKD animals may be associated with the decreased expression of mucin. Butyrate is known to increase the expression of mucin [17], TJ proteins [16] and CRAMP [39]. This study showed that butyrate treatment emended these parameters. To determine the reason for the decrease in Muc2 expression, we examined IL-10, since this cytokine can not only play an active role in colonic
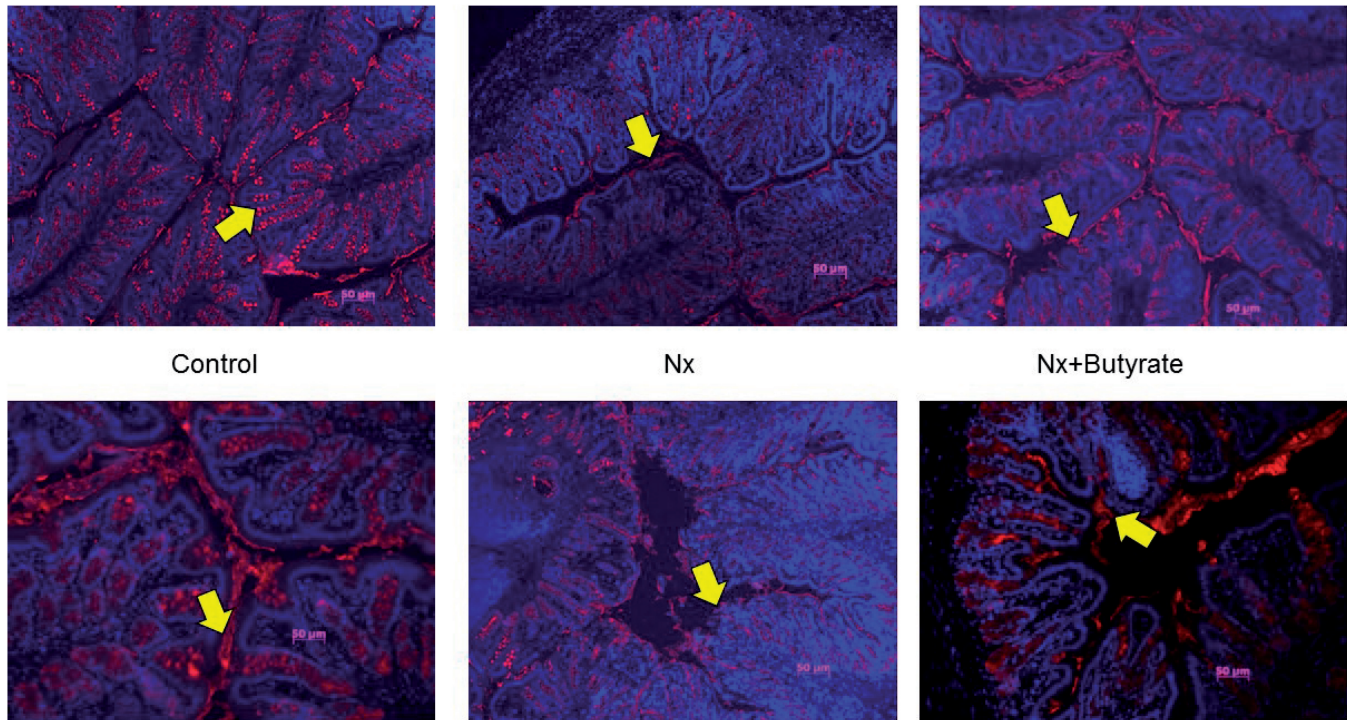
FIGURE 6: Muc2 expression in the colon analyzed immunohistochemically revealed decreased expression of Muc2 in the Nx group was abrogated by butyrate. Fluorescent microscopy of Muc2, stained red, merged with DNA-capturing 4′-6-diamidino-2-phenylindole, stained blue. Representative sections of colonic mucin of two animals from each group (control, Nx and butyrate-treated Nx) are shown. A total of six animals per group were used to assess Muc2 expression. The proximal part of the colon (0.5 cm) was collected and stored in Carnoy's solution. Muc2 expression was determined by immunohistochemistry using Muc2 antibody. The yellow arrow points to the Muc2 (red) expression. Compared with controls, Muc2 expression was significantly lower in the Nx groups. The butyrate-treated group had a significant increase in mucin expression.

Muc2 production in goblet cells [40, 41], but can also affect the integrity of the intestinal barrier [42]. Taken together, these findings demonstrate that downregulation of IL-10, as seen in the colon of CKD animals, and upregulation of IL-10 by butyrate may play a role in the changes of Muc2 expression and TJ proteins observed in this study. Vaziri *et al.* [7, 8] clearly demonstrated that there is a significant loss of TJ proteins of the gut in CKD animals, and this study further corroborates the earlier findings.

Phosphorylation of AMPK is necessary and important to maintain and strengthen mammalian epithelial TJs [43]. Therefore AMPK can also play a role in maintaining the integrity of TJ proteins. Loss of mucin and TJ proteins can lead to the leakage of uremic toxins such as LPS. Significant leakage of LPS in the circulation has been reported in other models of renal failure [5, 10]. *In vitro* studies with human colonic epithelial cells have shown that LPS can decrease the expression of TJ proteins and increase paracellular permeability [32]. In patients with different stages of CKD, there was a graduated increase of LPS levels and CKD progression that was associated with reduced survival and increased cardiac injury [44]. Our study shows a significant increase of LPS in the circulation of CKD rats. Butyrate abolished this increase by improving intestinal barrier function.

CAMKKβ can activate AMPK by phosphorylation [45]. Butyrate enhances intestinal barrier function [46] and activates AMPK by increasing its phosphorylation via CAMKKβ [16], which strengthens the intestine. This thereby reduces efflux of noxious material such as LPS.

CKD rats have been shown to have hyperglycemia, insulin resistance and impaired gluconeogenesis [28, 29]. Besides playing a role in strengthening the intestine, AMPK plays a significant role in energy homeostasis, and its effect on metabolism can modulate diabetes. Many natural compounds, such as resveratrol, produce antidiabetic effects by affecting AMPK [45]. We have observed a butyrate-mediated decrease in gluconeogenesis. Metformin, by activating AMPK, has been shown to decrease gluconeogenesis [47], although these findings have been challenged. A later study showed that activation of duodenal, but not hepatic, AMPK can prevent gluconeogenesis via signaling through a gut–brain–liver pathway [48]. Although we did not check for AMPK expression in the duodenum, the colonic expression was significantly activated by butyrate. By changing mitochondrial function [18] and histone deacetylase (HDAC) inhibition, butyrate treatment has been shown to improve insulin sensitivity and diabetes control [49]. Butyrate-mediated GLP-1 secretion has been considered to be a major factor in the improvement of insulin sensitivity and diabetes by probiotics [22]. GLP-1 has been shown to decrease hepatic gluconeogenesis and promote insulin secretion [50] and this can be an added factor by which butyrate could control hyperglycemia in CKD animals.
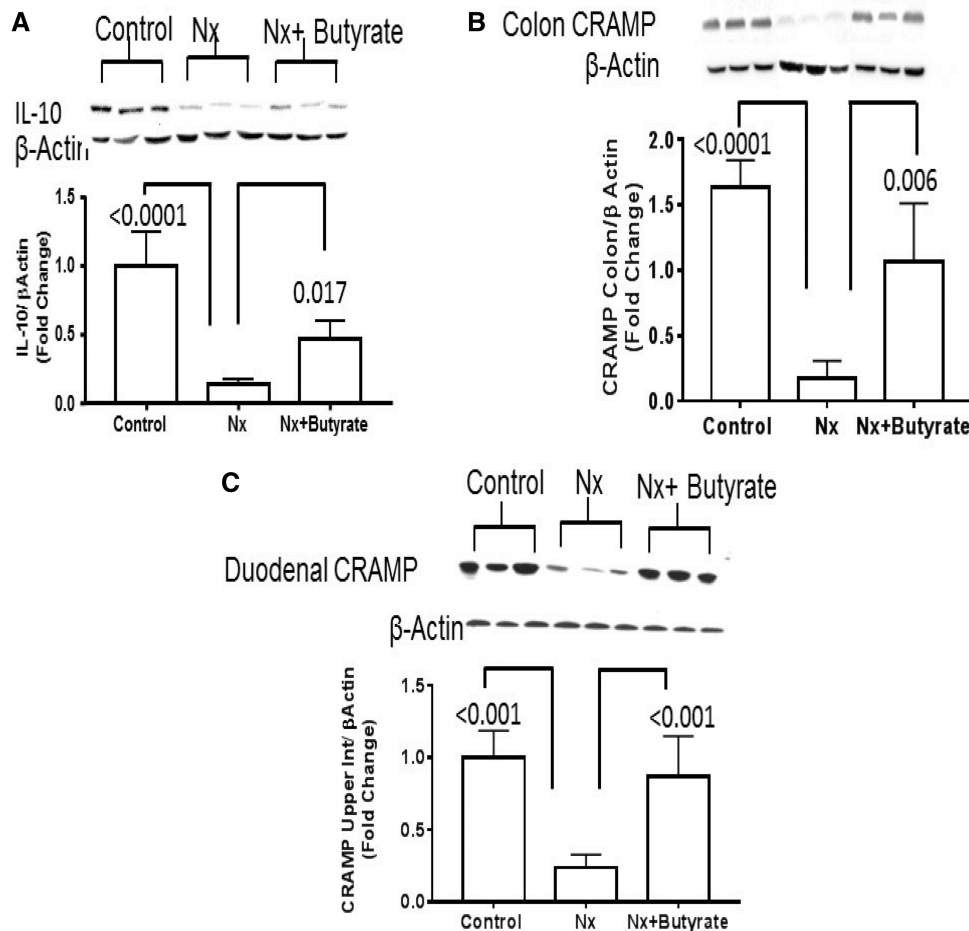
FIGURE 7: Butyrate treatment reversed the decrease of colonic IL-10 and duodenal CRAMP of Nx animals. **(A)** Representative western blot of IL-10 normalized to β-actin. Significant reduction of IL-10 in the colon of Nx animals reversed with butyrate; however, Nx + butyrate was significantly higher than in the control group (<0.001). **(B)** Representative western blot of colon CRAMP normalized to β-actin. **(C)** Representative western blot of duodenal CRAMP normalized to β-actin. Compared with the controls there was reduced expression of CRAMP in the colon and duodenum of Nx animals that was reversed with butyrate. Although butyrate treatment (Nx + butyrate) increased CRAMP expression in the colon, it was still significantly lower (P < 0.05) than in the control group. Only 50% of the colon from the Nx animals had detectable CRAMP. The expression of duodenal CRAMP in the Nx + butyrate and control groups was not significantly different. Data are mean ± standard deviation of six animals per group.

Table 1. Butyrate treatment decreased serum urea and proteinuria but did not significantly affect serum creatinine of Nx animals

	Control	Butyrate control	Nx	Nx + butyrate
Urea (mg/dL)	35.59 ± 4.48	32.18 ± 1.76	128.9 ± 23.43[a,b,c]	93.81 ± 18.75[a,b]
Urinary protein/urinary creatinine (fold change)	1.00 ± 0.20	1.36 ± 0.36	2.96 ± 0.81[a,b,c]	1.51 ± 0.7[a,d]
Creatinine (mg/dL)	0.3 ± 0.07	0.32 ± 0.09	0.97 ± 0.17[a,b]	0.7 ± 0.17[a,b]

Nx animals had significantly higher serum urea than the controls. This increase was reduced by butyrate treatment. Proteinuria, measured as the ratio of urinary protein to urinary creatinine, was significantly higher in Nx rats. Butyrate treatment significantly reduced proteinuria. The Nx cohort had significantly higher creatinine than the controls. Butyrate treatment did not significantly reduce serum creatinine (P = 0.0504). Data are mean ± standard deviation of six animals per group. The butyrate control group had five animals. Statistically significant differences between the groups are given as follows:

[a]P < 0.001 compared with control.
[b]P < 0.001 compared with butyrate control.
[c]P < 0.01 compared with Nx + butyrate.
[d]P < 0.05 compared with butyrate control.

Elevated serum urea and proteinuria were reduced by butyrate, which leads us to conclude that butyrate has a mild to moderate effect on renal failure. However, it did not have a significant effect on serum creatinine (P = 0.0504). It is also possible that the alleviation of renal failure could be secondary to the improvement of metabolic parameters (glucose tolerance, insulin tolerance and gluconeogenesis). However, it should be noted that a high fermentable fiber diet can be used by the gut microbiome to produce SCFAs (acetate, propionate and butyrate) and such a diet has been shown to improve renal failure [25,

26]. It is possible than an increased dosage of butyrate or a mixture of fatty acids could have a greater impact in ameliorating renal failure. This is a limitation that needs to be elucidated. Another limitation of this study was that the butyrate uptake in the colon was not monitored. Since butyrate can be absorbed from the small intestine, there is a possibility that the effect of butyrate may not be completely restricted to the colon and a systemic response cannot be ruled out. In a recent study, it was found that Chinese patients with ESRD have reduced levels of butyrate-producing bacteria [51]. Thus butyrate and butyrate-producing bacteria may play a role in CKD, especially in patients with renal failure with diabetes. It is noteworthy that ESRD patients have lower levels of SCFA-producing bacteria in their gut [20].

This study has shown that the intestine can play a major role in aggravating renal failure and diabetes. We have shown some of the mechanisms by which butyrate can affect intestinal permeability. There are other functions of butyrate, such as HDAC inhibition, that may also play a role in intestinal permeability and need to be investigated.

CONFLICT OF INTEREST STATEMENT

None declared.

REFERENCES

1. Anders HJ, Andersen K, Stecher B. The intestinal microbiota, a leaky gut, and abnormal immunity in kidney disease. *Kidney Int* 2013; 83: 1010–1016
2. Nallu A, Sharma S, Ramezani A *et al*. Gut microbiome in chronic kidney disease: challenges and opportunities. *Transl Res* 2017; 179: 24–37
3. Vaziri ND, Wong J, Pahl M *et al*. Chronic kidney disease alters intestinal microbial flora. *Kidney Int* 2013; 83: 308–315
4. Cani PD, Osto M, Geurts L *et al*. Involvement of gut microbiota in the development of low-grade inflammation and type 2 diabetes associated with obesity. *Gut Microbes* 2012; 3: 279–288
5. Ghosh SS, Righi S, Krieg R *et al*. High fat high cholesterol diet (western diet) aggravates atherosclerosis, hyperglycemia and renal failure in nephrectomized LDL receptor knockout mice: role of intestine derived lipopolysaccharide. *PLoS One* 2015; 10: e0141109
6. Vaziri ND, Zhao YY, Pahl MV. Altered intestinal microbial flora and impaired epithelial barrier structure and function in CKD: the nature, mechanisms, consequences and potential treatment. *Nephrol Dial Transplant* 2016; 31: 737–746
7. Vaziri ND, Yuan J, Nazertehrani S *et al*. Chronic kidney disease causes disruption of gastric and small intestinal epithelial tight junction. *Am J Nephrol* 2013; 38: 99–103
8. Vaziri ND, Yuan J, Rahimi A *et al*. Disintegration of colonic epithelial tight junction in uremia: a likely cause of CKD-associated inflammation. *Nephrol Dial Transplant* 2012; 27: 2686–2693
9. Johansson ME, Hansson GC. Immunological aspects of intestinal mucus and mucins. *Nat Rev Immunol* 2016; 16: 639–649
10. Andersen K, Kesper MS, Marschner JA *et al*. Intestinal dysbiosis, barrier dysfunction, and bacterial translocation account for CKD-related systemic inflammation. *J Am Soc Nephrol* 2017; 28: 76–83
11. Cornick S, Tawiah A, Chadee K. Roles and regulation of the mucus barrier in the gut. *Tissue Barriers* 2015; 3: e982426
12. McGuckin MA, Lindén SK, Sutton P *et al*. Mucin dynamics and enteric pathogens. *Nat Rev Microbiol* 2011; 9: 265–278
13. Louis P, Hold GL, Flint HJ. The gut microbiota, bacterial metabolites and colorectal cancer. *Nat Rev Microbiol* 2014; 12: 661–672
14. Sharon G, Garg N, Debelius J *et al*. Specialized metabolites from the microbiome in health and disease. *Cell Metab* 2014; 20: 719–730
15. Leonel AJ, Alvarez-Leite JI. Butyrate: implications for intestinal function. *Curr Opin Clin Nutr Metab Care* 2012; 15: 474–479
16. Miao W, Wu X, Wang K *et al*. Sodium butyrate promotes reassembly of tight junctions in Caco-2 monolayers involving inhibition of MLCK/MLC2 pathway and phosphorylation of PKCβ2. *Int J Mol Sci* 2016; 17: 1696
17. Finnie IA, Dwarakanath AD, Taylor BA *et al*. Colonic mucin synthesis is increased by sodium butyrate. *Gut* 1995; 36: 93–99
18. Gao Z, Yin J, Zhang J *et al*. Butyrate improves insulin sensitivity and increases energy expenditure in mice. *Diabetes* 2009; 58: 1509–1517
19. Khan S, Jena G. Sodium butyrate reduces insulin-resistance, fat accumulation and dyslipidemia in type-2 diabetic rat: a comparative study with metformin. *Chem Biol Interact* 2016; 254: 124–134
20. Wong J, Piceno YM, DeSantis TZ *et al*. Expansion of urease- and uricase-containing, indole- and p-cresol-forming and contraction of short-chain fatty acid-producing intestinal microbiota in ESRD. *Am J Nephrol* 2014; 39: 230–237
21. Ramezani A, Raj DS. The gut microbiome, kidney disease, and targeted interventions. *J Am Soc Nephrol* 2014; 25: 657–670
22. Yadav H, Lee JH, Lloyd J *et al*. Beneficial metabolic effects of a probiotic via butyrate-induced GLP-1 hormone secretion. *J Biol Chem* 2013; 288: 25088–25097
23. Zavattaro M, Caputo M, Samà MT *et al*. One-year treatment with liraglutide improved renal function in patients with type 2 diabetes: a pilot prospective study. *Endocrine* 2015; 50: 620–626
24. von Scholten BJ, Hansen TW, Goetze JP *et al*. Glucagon-like peptide 1 receptor agonist (GLP-1 RA): long-term effect on kidney function in patients with type 2 diabetes. *J Diabetes Complicat* 2015; 29: 670–674
25. Kieffer DA, Piccolo BD, Vaziri ND *et al*. Resistant starch alters gut microbiome and metabolomic profiles concurrent with amelioration of chronic kidney disease in rats. *Am J Physiol Renal Physiol* 2016; 310: F857–F871
26. Vaziri ND, Liu SM, Lau WL *et al*. High amylose resistant starch diet ameliorates oxidative stress, inflammation, and progression of chronic kidney disease. *PLoS One* 2014; 9: e114881
27. Yang HC, Zuo Y, Fogo AB. Models of chronic kidney disease. *Drug Discov Today Dis Models* 2010; 7: 13–19
28. Chapagain A, Caton PW, Kieswich J *et al*. Elevated hepatic 11β-hydroxysteroid dehydrogenase type 1 induces insulin resistance in uremia. *Proc Natl Acad Sci USA* 2014; 111: 3817–3822
29. Hosoya K, Minakuchi H, Wakino S *et al*. Insulin resistance in chronic kidney disease is ameliorated by spironolactone in rats and humans. *Kidney Int* 2015; 87: 749–760
30. Lin HV, Frassetto A, Kowalik EJ *et al*. Butyrate and propionate protect against diet-induced obesity and regulate gut hormones via free fatty acid receptor 3-independent mechanisms. *PLoS One* 2012; 7: e35240
31. Ghosh SS, Massey HD, Krieg R *et al*. Curcumin ameliorates renal failure in 5/6 nephrectomized rats: role of inflammation. *Am J Physiol Renal Physiol* 2009; 296: F1146–F1157
32. Ghosh SS, Bie J, Wang J *et al*. Oral supplementation with non-absorbable antibiotics or curcumin attenuates western diet-induced atherosclerosis and glucose intolerance in LDLR-/- mice – role of intestinal permeability and macrophage activation. *PLoS One* 2014; 9: e108577
33. Ghosh SS, Krieg R, Massey HD *et al*. Curcumin and enalapril ameliorate renal failure by antagonizing inflammation in 5/6 nephrectomized rats: role of phospholipase and cyclooxygenase. *Am J Physiol Renal Physiol* 2012; 302: F439–F454
34. Kameyama A, Dong W, Matsuno YK. Succinylation-Alcian blue staining of mucins on polyvinylidene difluoride membranes. *Methods Mol Biol* 2015; 1314: 325–331
35. Huang Y, de Boer WB, Adams LA *et al*. Image analysis of liver collagen using sirius red is more accurate and correlates better with serum fibrosis markers than trichrome. *Liver Int* 2013; 33: 1249–1256
36. Cani PD, Amar J, Iglesias MA *et al*. Metabolic endotoxemia initiates obesity and insulin resistance. *Diabetes* 2007; 56: 1761–1772

37. Guttman JA, Finlay BB. Tight junctions as targets of infectious agents. *Biochim Biophys Acta* 2009; 1788: 832–841
38. Joshi S, Kumar S, Bafna S *et al.* Genetically engineered mucin mouse models for inflammation and cancer. *Cancer Metastasis Rev* 2015; 34: 593–609
39. Cobo ER, Kissoon-Singh V, Moreau F *et al.* MUC2 mucin and butyrate contribute to the synthesis of the antimicrobial peptide cathelicidin in response to *Entamoeba histolytica*- and dextran sodium sulfate-induced colitis. *Infect Immun* 2017; 85
40. Hasnain SZ, Tauro S, Das I *et al.* IL-10 promotes production of intestinal mucus by suppressing protein misfolding and endoplasmic reticulum stress in goblet cells. *Gastroenterology* 2013; 144: 357–368.e359
41. Schwerbrock NM, Makkink MK, van der Sluis M *et al.* Interleukin 10-deficient mice exhibit defective colonic Muc2 synthesis before and after induction of colitis by commensal bacteria. *Inflamm Bowel Dis* 2004; 10: 811–823
42. Sun X, Yang H, Nose K *et al.* Decline in intestinal mucosal IL-10 expression and decreased intestinal barrier function in a mouse model of total parenteral nutrition. *Am J Physiol Gastrointest Liver Physiol* 2008; 294: G139–G147
43. Aznar N, Patel A, Rohena CC *et al.* AMP-activated protein kinase fortifies epithelial tight junctions during energetic stress via its effector GIV/Girdin. *Elife* 2016; 5: e20795
44. McIntyre CW, Harrison LE, Eldehni MT *et al.* Circulating endotoxemia: a novel factor in systemic inflammation and cardiovascular disease in chronic kidney disease. *Clin J Am Soc Nephrol* 2011; 6: 133–141
45. Hardie DG. AMPK: a target for drugs and natural products with effects on both diabetes and cancer. *Diabetes* 2013; 62: 2164–2172
46. Peng L, Li ZR, Green RS *et al.* Butyrate enhances the intestinal barrier by facilitating tight junction assembly via activation of AMP-activated protein kinase in Caco-2 cell monolayers. *J Nutr* 2009; 139: 1619–1625
47. Zhou G, Myers R, Li Y *et al.* Role of AMP-activated protein kinase in mechanism of metformin action. *J Clin Invest* 2001; 108: 1167–1174
48. Duca FA, Côté CD, Rasmussen BA *et al.* Metformin activates a duodenal AMPK-dependent pathway to lower hepatic glucose production in rats. *Nat Med* 2015; 21: 506–511
49. Khan S, Jena G. The role of butyrate, a histone deacetylase inhibitor in diabetes mellitus: experimental evidence for therapeutic intervention. *Epigenomics* 2015; 7: 669–680
50. Jin T, Weng J. Hepatic functions of GLP-1 and its based drugs: current disputes and perspectives. *Am J Physiol Endocrinol Metab* 2016; 311: E620–E627
51. Jiang S, Xie S, Lv D *et al.* Alteration of the gut microbiota in Chinese population with chronic kidney disease. *Sci Rep* 2017; 7: 2870

Delayed spironolactone administration prevents the transition from acute kidney injury to chronic kidney disease through improving renal inflammation

Jonatan Barrera-Chimal[1,2], Leslie Rocha[1,3], Isabel Amador-Martínez[1,2], Rosalba Pérez-Villalva[1,3], Rafael González[1,3], Cesar Cortés-González[4], Norma Uribe[5], Victoria Ramírez[3], Nathan Berman[1,3], Gerardo Gamba[1,3] and Norma A. Bobadilla[1,3]

[1]Molecular Physiology Unit, Department of Genomic Medicine, Instituto de Investigaciones Biomédicas, Universidad Nacional Autónoma de México, Mexico City, Mexico, [2]Unidad de Medicina Traslacional, Department of Genomic Medicine, Instituto de Investigaciones Biomédicas and Instituto Nacional de Cardiología Ignacio Chávez, Mexico City, Mexico, [3]Department of Nephrology Instituto Nacional de Ciencias Médicas y Nutrición Salvador Zubirán, Mexico City, Mexico, [4]Unidad de Investigación Biomédica en Cáncer, Instituto Nacional de Cancerología, Mexico City, Mexico and [5]Department of Pathology, Instituto Nacional de Ciencias Médicas y Nutrición Salvador Zubirán, Mexico City, Mexico

Correspondence and offprint requests to: Norma A. Bobadilla; E-mail: nab@biomedicas.unam.mx

ABSTRACT

Background. Acute kidney injury (AKI) is not as harmless as previously thought since it may lead to chronic kidney disease (CKD). Because most of the time ischemic AKI occurs unexpectedly, it is difficult to prevent its occurrence and there are no specific therapeutic approaches to prevent the AKI to CKD transition. We aimed to determine whether mineralocorticoid receptor blockade (MRB) in the first days after ischemia/reperfusion (IR) can prevent progression to CKD.

Methods. Four groups of male Wistar rats were included: sham and three groups of bilateral renal ischemia for 45 min, one without treatment and the other two receiving spironolactone for 5 or 10 days, starting 24 h after IR. The rats were studied at 10 days or 5 months after ischemia induction.

Results. After 5 months of follow-up, the untreated group exhibited clear evidence of AKI to CKD progression, such as proteinuria, reduced renal blood flow, tubulointerstitial fibrosis, glomerulosclerosis and glomerular hypertrophy. All these alterations were prevented by both spironolactone treatments initiated 24 h after IR, the 10-day treatment being more effective. Within the early mechanisms of the MRB protective effect are the reduction of inflammation and increased endothelin-B-receptor expression and endothelial nitric oxide synthase activation in the first 10 days after IR.